# Efficient implementation of WENO Scheme on structured meshes

o Xinrong Su, Dept. Aero. Enging, Tohoku Univ, Sendai, E-mail: su@ad.mech.tohoku.ac.jp
Daisuke Sasaki, Dept. Aero. Enging, Tohoku Univ, Sendai, E-mail: sasaki@ad.mech.tohoku.ac.jp
Kazuhiro Nakahashi, Dept. Aero. Enging, Tohoku Univ, Sendai, E-mail: naka@ad.mech.tohoku.ac.jp

In this paper the application of high order Weighted Essentially Nonoscillatory (WENO) reconstruction to the subsonic and transonic engineering problems is studied. It is observed the WENO scheme based on the characteristic variable has better convergence speed and accuracy than the WENO scheme based on primitive variable. For engineering problems with shock of moderate amplitude, a simplified version of the characteristic variable based WENO with which the CPU cost overhead can be significantly reduced is developed. Also in this work it is found for viscous case it is better to include the viscous effect which is reflected by the modification to a parameter in the WENO reconstruction. Numerical results indicate with the use of the simplified characteristic variable based reconstruction and the modified parameter, the nonlinear WENO interpolation is sharply activated in the region of shock jump and meanwhile in the smooth area the WENO interpolation weights are tuned towards the designed optimal value for better accuracy. Also this approach demonstrates better convergence rate than the primitive variable based reconstruction. Several practical cases are calculated to demonstrate the accuracy and efficiency of the current methodology.

## 1. Introduction

It is well known computational fluid dynamics (CFD) offers the ability to perform predictions of the full field vehicle flows at low cost compared to wind tunnel experiments. While the accurate and fast-turnaround simulation still demands new algorithms. Up to now, the widely used codes for engineering problems employ second-order schemes. Higher order numerical methods, such as the Weighted Essentially Nonoscillatory and Discontinuous Galerkin (DG), can provide more accurate solutions with fewer mesh points. In the higher order schemes, the numerical dissipation is reduced and this is one of the key elements of accurate capture of detailed flow structures, such as tip vortex and shock-vortex interaction. Currently most of the efforts are exerted in the application of these methods in the field of high-fidelity simulations, such as large eddy simulation (LES) and aeroacoustics. While high order schemes are rarely applied to engineering problems, such as wing-body and turbomachinery cases. Compared to the lower order numerical schemes, high accuracy schemes are CPU extensive. Due to the more stencils needed for high accuracy and reduced numerical dissipation, these methods are always numerically stiff and usually exhibit slower convergence speed and reduced stability.

Of all the high order schemes, Essentially Nonoscillatory (ENO) and WENO algorithms can be used to replace the widely used Monotone Upwind Scheme for Conservation Laws (MUSCL)[1] approach in structured codes for more accurate inviscid fluxes. In the ENO approach, several candidate reconstruction stencils are formed and the nonoscillatory property is achieved by selecting the one with maximum smoothness. In this approach the stencil interpolated across the discontinuity are never used and the oscillations are prevented. Based on the ENO algorithm, Liu et al.[2] developed the WENO scheme by the convex combination of all the stencils to improve the accuracy. In the WENO algorithm, the stencil interpolated across the discontinuity is assigned a near zero weight and thus the nonoscillation property is preserved. Jiang and Shu[3] further developed the WENO algorithm by devising a new set of weights for higher accuracy. Currently the WENO algorithm is widely used in the high fidelity simulations. Especially in the simulation of shock-turbulence interactions, it serves as the building part to capture the shock without dissipating the small scale turbulent fluctuations[4]. Ren et al.[5] developed a Roe type characteristic-wise hybrid compact-WENO scheme in which compact difference is used in the smooth regions and the WENO scheme is activated near the shock by a weight function. Zhang and Shu[6] proposed a new smoothness indicator to improve the convergence issue of WENO scheme to steady state.

Compared to the extensive researches and applications in high fidelity simulations, the use of WENO scheme in the engineering problems are less studied. Nichols et al.[7] applied the fifth order WENO in the NASA OVERFLOW code and tested the scheme with problems involving vortical flows, strong shock and large scale unsteady flows. The WENO scheme was found to provide much lower numerical dissipation and dispersion compared to the widely used third order MUSCL reconstruction. Shen et al.[8] studied the weights stability and accuracy of fifth order WENO scheme. It is found the weight of the original WENO scheme may lead to oscillation even for smooth flows. According to numerical experiments, it is proposed to increase a parameter from $10^{-6}$ to $10^{-2}$ and the convergence property and the accuracy can be significantly improved.

In this paper the authors are interested in how to efficiently apply the WENO reconstruction to engineering problems for better accuracy. Also the numerical method should have favorable convergence speed for steady state solutions. In the literature[7,8,9], for engineering problems using either WENO or MUSCL type reconstruction, it is believed there is no need to resort to the expensive characteristic variable based reconstruction. While in this paper it is found the use of characteristic variable helps to improve the accuracy and convergence speed. Also for the transonic problems interested in this paper, a simplified version can be used to obviously reduce the cost overhead in the characteristic variable based approach. The application of WENO scheme can be further improved by taking into account of the viscous effect. With the use of characteristic variable and the consideration of viscous effect, the current implementation tends to sharply activate the nonlinear interpolation near the shock for

monotone solution. At the same time in the smooth area the unnecessary nonlinear interpolation is suppressed. Also the current implementation has similar or better convergence rate than the primitive variable based WENO. Several practical engineering problems are used to validate the accuracy and convergence issues of the current method.

## 2. Numerical methods

The governing equation can be written in the Cartesian coordinate as

$$\frac{\partial U}{\partial t}+\frac{\partial F}{\partial x}+\frac{\partial G}{\partial y}+\frac{\partial H}{\partial z}=0$$

in which $U=[\rho,\rho u,\rho v,\rho w,\rho E]^T$ denotes the conservative variable. $F,G,H$ denote the convective fluxes and also include viscous fluxes for viscous cases. Also the primitive variable $W=[\rho,u,v,w,p]^T$ is widely used in this work. The governing equation is nondimensionalized with the freestream conditions and proper length scale.

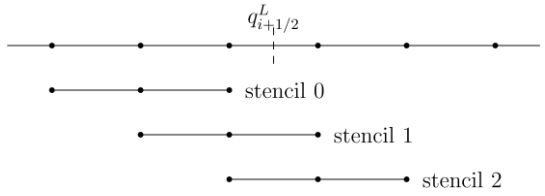


Fig. 1 Reconstruction stencils for the fifth order WENO algorithm

The reconstruction of variables with WENO method provides a method to achieve higher order accuracy both in the smooth part and in the shock part of flow region, compared to the currently widely used MUSCL approach. In the WENO method, the essentially non-oscillation and high order accuracy properties are realized by the convex and nonlinear combination of several low order approximations. As demonstrated in Fig. 1, the fifth-order accurate WENO reconstruction of $q^L_{i+1/2}$ can be written as

$$q^L_{i+1/2}=\omega_0 q_0+\omega_1 q_1+\omega_2 q_2$$

where

$$\begin{cases} q_0=\frac{1}{3}q_{i-2}-\frac{7}{6}q_{i-1}+\frac{11}{6}q_i \\ q_1=-\frac{1}{6}q_{i-1}+\frac{5}{6}q_i+\frac{1}{3}q_{i+1} \\ q_2=\frac{1}{3}q_i+\frac{5}{6}q_{i+1}-\frac{1}{6}q_{i+2} \end{cases}$$

and the weights are defined as

$$\omega_s=\frac{\alpha_s}{\sum\alpha_s},\alpha_s=\frac{C_s}{\epsilon+IS_s} \qquad (1)$$

. In the above equation, the smoothness indicators $IS_s$ are

$$\begin{cases} IS_0=\frac{13}{12}(q_{i-2}-2q_{i-1}+q_i)^2+\frac{1}{4}(q_{i-2}-4q_{i-1}+3q_i)^2 \\ IS_1=\frac{13}{12}(q_{i-1}-2q_i+q_{i+1})^2+\frac{1}{4}(q_{i-1}-q_{i+1})^2 \\ IS_2=\frac{13}{12}(q_i-2q_{i+1}+q_{i+1})^2+\frac{1}{4}(3q_i-4q_{i+1}+q_{i+2})^2 \end{cases}$$

and up-to-now the calculation of $q^L_{i+1/2}$ is completed and $q^R_{i+1/2}$ can be constructed in the way symmetric to $q^L_{i+1/2}$ and will not be detailed here. In the shock region, the reconstruction stencil across the shock will be assigned a small weight and now the interpolation is a nonlinear process. In the smooth area, all the weights approach the designed optimal values and linear interpolation is used indeed.

There are several choices of the variable to be reconstructed, such as the primitive variable, conservative variable, or the characteristic variable. Currently in most of the engineering cases using the WENO algorithm, the WENO reconstruction is used either to the conservative variables[8], or to the primitive variables[7,9]. As conservative variable and primitive variable are always available in the code and thus these methods are straightforward. Another approach is to use the WENO method in the characteristic field. Let $(n_x,n_y,n_z)^T$ be an unit length vector of the surface normal, the Jacobian matrix is defined as

$$\frac{\partial F_n}{\partial U}=\frac{\partial(Fn_x+Gn_y+Hn_z)}{\partial U}$$

, also denotes $R$ and $L$ the right and left eigenmatrix of the above matrix, respectively. In the calculation of $U^L_{i+1/2}$ and $U^R_{i+1/2}$, the conservative variables are multiplied by the left eigenmatrix $L$ to get the characteristic variables $\mathcal{L}$. Then the WENO reconstruction is used to calculate $\mathcal{L}^L_{i+1/2}$ and $\mathcal{L}^R_{i+1/2}$. The last step is the transformation from characteristic variable to conservative variable by

$$U^L_{i+1/2}=R\mathcal{L}^L_{i+1/2},U^R_{i+1/2}=R\mathcal{L}^R_{i+1/2}$$

. Compared to the methods based on the conservative variable and primitive variable, in the characteristic variable based approach, the left and right eigenmatrices have to be formed and also matrix-vector multiplications are needed. These result in obvious CPU cost overhead. Also in the literature it is believed for engineering problems with high order reconstructions, such as the fifth order WENO scheme, the using of characteristic variable does not result in additional gains. As a result it is seldom used in engineering problems for these two reasons.

In the following the characteristic variable will be computed from primitive variable, as the transformations are much simplified compared to from conservative variable. The governing equation can be transformed into

$$\frac{\partial U}{\partial W}\frac{\partial W}{\partial t}+\frac{\partial F}{\partial W}\frac{\partial W}{\partial x}+\frac{\partial G}{\partial W}\frac{\partial W}{\partial y}+\frac{\partial H}{\partial W}\frac{\partial W}{\partial z}=0$$

. The Jacobian matrix and the eigenvalue decomposition are defined as

$$A_W=\frac{\partial W}{\partial U}\left(n_x\frac{\partial F}{\partial W}+n_y\frac{\partial G}{\partial W}+n_z\frac{\partial H}{\partial W}\right)=R_W\Lambda L_W$$

. For clarity, two dimensional case will be discussed here. Denoting $\mathbf{m}=(m_x,m_y)^T$ a unit vector which is perpendicular to $\mathbf{n}=(n_x,n_y)^T$, the left eigenmatrix can be described in the form of

$$L_W=\begin{bmatrix} 1 & 0 & 0 & -\frac{1}{a^2} \\ 0 & \frac{\rho n_x}{2a} & \frac{\rho n_y}{2a} & \frac{1}{2a^2} \\ 0 & -\frac{\rho n_x}{2a} & -\frac{\rho n_y}{2a} & \frac{1}{2a^2} \\ 0 & \rho m_x & \rho m_y & 0 \end{bmatrix}$$

. As shown in Eqn. (1), in the WENO algorithm, the smoothness is estimated by the variations of the variables to be reconstructed.

Thus looking at the characteristic variable based WENO algorithm, $L_W \delta W$ has the form of

$$L_W \delta W = \begin{bmatrix} \frac{a^2\delta\rho - \delta p}{a^2} & \frac{\delta p \pm \rho a \delta u_n}{2a^2} & \rho \delta u_m \end{bmatrix}^T \quad (2)$$

. The first component of $L_W \delta W$ represents the entropy wave and the second and the third component represents the downstream and upstream propagating pressure wave, respectively. The last one represents the shear wave, viz., vorticity. Compared to the primitive variable or conservative variable, the characteristic variable better reflects the flow features. For example in the isentropic flow, $\delta p = a^2 \delta \rho$. So if characteristic variable based WENO reconstruction is used, according to the definition of the WENO weights in Eqn. (1), linear interpolation instead of the lower order nonlinear interpolation will be used in this characteristic field. While for the same case, due to the variations of $\rho$ and $p$, the primitive variable and the conservative variable based approaches tend to activate the low order nonlinear interpolations despite the shockless flow.

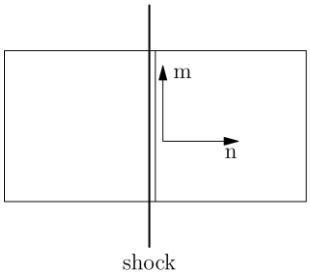


Fig. 2 Case with shock wave aligned with the grid

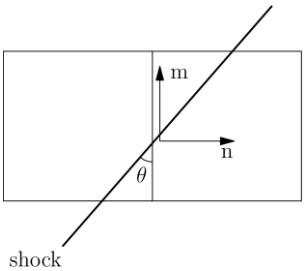


Fig. 3 Case with shock wave not aligned with the grid

Obviously the first three components in Eqn. (2) vary significantly across the shock, while the variation of the last component is a bit different. As demonstrated in the Fig. 2, in the case of the shock wave is aligned with the grid, according to the Rankine-Hugoniot conditions, the velocity difference in the tangential direction vanishes $\delta u_m = 0$. Thus the last component approaches zero and at least there is no need to use the nonlinear WENO interpolation to suppress the spurious oscillation in this characteristic field. In the case the shock wave is not aligned with the grid lines, as depicted in Fig. 3, the velocity difference tangential to the shock wave is zero and does not contribute to $\delta u_m$. Denoting the velocity component normal to the shock wave as $u_{\text{norm}}$, in this case $\delta u_m$ can be expressed as

$$\delta u_m = -\delta u_{\text{norm}} \sin\theta$$

For the engineering problems interested in this paper, the shock wave is of moderate amplitude and according to the Rankine-Hugoniot conditions $\delta u_{\text{norm}}$ is a limited value. Also in the generation of structured mesh, the mesh lines are always positioned to be aligned with the dominate flow features, such as shock waves and boundary layers. Thus for high quality mesh $\theta$ is always a small angle. So in the case the shock wave is not aligned with the grid lines, for transonic flows calculated with structured meshes, there is always no need to use the nonlinear and also expensive WENO interpolation to the component of the characteristic variable corresponding to the vorticity wave. For three dimensional problems similar analysis also applies and will not be repeated here and in three dimensions the two components corresponding to the vorticity waves can be omitted in the WENO reconstruction.

As a result for these cases a simplified version of the characteristic variable based WENO reconstruction can be introduced. Denoting $L^j$ as the j-th row of $L_W$ and $R^j$ the j-th column$R_W$. For both two and three dimensional problems, the nonlinear WENO interpolation is needed only for the first three components of characteristic variable, while linear reconstruction is used for the remaining part. The reconstruction is executed in the following steps: (1). Compute $W_{i+1/2}$ from $W_i$ and $W_{i+1}$ and then calculate $L^j, R^j, j = 1,2,3$. (2). Primitive variable is transformed into characteristic form by $\mathcal{L}^j = L^j W, j = 1,2,3$ and WENO reconstruction is used to compute $\mathcal{L}^{j,L}_{i+1/2}$ and $\mathcal{L}^{j,R}_{i+1/2}, j = 1,2,3$ . (3). Denoting the remaining part as $\mathcal{W} = W - \sum_{j=1}^{3} R^j \mathcal{L}^j$, linear reconstruction is used for this part.

For third order accuracy, the reconstruction has the form of

$$\mathcal{W}^L_{i+1/2} = -\frac{1}{6}\mathcal{W}_{i-1} + \frac{5}{6}\mathcal{W}_i + \frac{1}{3}\mathcal{W}_{i+1}$$
$$\mathcal{W}^R_{i+1/2} = \frac{1}{3}\mathcal{W}_i + \frac{5}{6}\mathcal{W}_{i+1} - \frac{1}{6}\mathcal{W}_{i+2}$$

. For fifth order accuracy the reconstruction can be expressed as

$$\mathcal{W}^L_{i+1/2} = \frac{1}{30}\mathcal{W}_{i-2} - \frac{13}{60}\mathcal{W}_{i-1} + \frac{47}{60}\mathcal{W}_i + \frac{9}{20}\mathcal{W}_{i+1} - \frac{1}{20}\mathcal{W}_{i+2}$$
$$\mathcal{W}^R_{i+1/2} = \frac{1}{30}\mathcal{W}_{i+3} - \frac{13}{60}\mathcal{W}_{i+2} + \frac{47}{60}\mathcal{W}_{i+1} + \frac{9}{20}\mathcal{W}_i - \frac{1}{20}\mathcal{W}_{i-1}$$

(4). The last step is to get $W^L_{i+1/2}$ and $W^R_{i+1/2}$ by summing up the two parts

$$W^L_{i+1/2} = \mathcal{W}^L_{i+1/2} + \sum_{j=1}^{3} R^j \mathcal{L}^{j,L}_{i+1/2}$$
$$W^R_{i+1/2} = \mathcal{W}^R_{i+1/2} + \sum_{j=1}^{3} R^j \mathcal{L}^{j,R}_{i+1/2}$$

Compared with the original implementation of characteristic variable base WENO reconstruction, the current simplified version obviously yields reduced computation cost. As only $L^i, i = 1,2,3$ and $R^i, i = 1,2,3$ instead of the full matrices have to be formed and also the count of matrix-vector multiplications used to calculate the characteristic variable has been reduced. And also the costly WENO algorithm is needed only for the first three components of the characteristic variable, instead of all the four components in two dimensions or five components in three dimensions.

For transonic flows in the engineering regime, there is a slightly rise of vorticity magnitude across shock wave, while the vorticity increases rapidly in the region with high velocity shear, such as in the boundary layer and the tip vortex region. The requirement of accurate tracking vorticity along long distance is necessary in many engineering problems. While due to the inherent numerical viscosity in numerical schemes, the vorticity is always dissipated much earlier[9]. In the current simplified WENO algorithm, linear reconstruction is used for the components corresponding to the vorticity waves, thus the numerical dissipation is further reduced and better accuracy for vortical flows is possible.

The WENO reconstruction algorithm computes several low-order approximations of $q^L_{i+1/2}$ and $q^R_{i+1/2}$ and the final value is obtained by the weighted summation of all the low-order approximations. This process is nonlinear and the weights are directly related to the smoothness indicators. As seen in Eqn. (1), the weight is determined by the ratio of its smoothness relative to the total smoothness. Thus there may be situation in which the absolute variation of $q$ is small, while the relative variation of $q$ is bigger. In this case the reconstruction stencil with relatively large variation will be assigned a small weight, no matter whether the shock wave do exists. Also during the transient stage from initial solution to the final converged solution, there is always small amplitude variation even in the subsonic area, in this case the smoothness indicators will work unreasonably and this may hinder the time marching towards convergence. According to Eqn. (1), if $IS_s \ll \epsilon$, the weights always approach the designed optimal values despites of the smoothness indicators. Thus although the small value $\epsilon$ in Eqn. (1) is originally designed to avoid the denominator from zero, in real-world problems, $\epsilon$ acts as a threshold to distinguish the acceptable small amplitude variation from the shock wave. In the smooth area, it is better to have $\epsilon$ on the same order or bigger than $IS_s$ so the designed order of accuracy can be achieved, while near the shock $\epsilon$ should be much smaller than $IS_s$ to activate the shock capturing. In the original WENO algorithm, $\epsilon$ is set to $10^{-6}$. In the work of Shen *et al.*[8], according to numerical experiments, this value is increased to $10^{-2}$. It is hard to define a value suitable for broad range of flows, while it is believed using a bigger $\epsilon$ which also does not destroy the shock capturing ability is beneficial for both accuracy and convergence. Similar as in the work of Shen *et al.*[8], in this paper $\epsilon$ is set to $10^{-2}$.

Note that for smooth flows $IS_s$ should converge to zero with mesh refinement; while for the reconstruction stencil across the shock wave, $IS_s$ converges to a finite value with mesh refinement. So it is better to have the parameter $\epsilon$ to be function of the local mesh spacing. For general cases it is a hard job and in this work the effect of local mesh spacing is considered in a more physical manner. In all the above discussions, only the inviscid part in concerned. For viscous flows, the viscosity, including the molecular part and the turbulent part, helps to stabilize the calculation and smooth the flow field. So taking into account of the physical viscosity would better suit the physical process. For simplicity, looking at a one dimensional convective-diffusion equation

$$\frac{\partial f}{\partial t} + a\frac{\partial f}{\partial x} = \mu\frac{\partial^2 f}{\partial x^2}$$

. This equation is semi-discretized as

$$\frac{\partial f}{\partial t} = -a\frac{f_{i+1} - f_{i-1}}{2\delta x} + \mu\frac{u_{i+1} - 2u_i + u_{i-1}}{\delta x^2}$$
$$= \left(\frac{\mu}{\delta x^2} - \frac{a}{2\delta x}\right)(u_{i+1} - u_i) + \left(\frac{\mu}{\delta x^2} + \frac{a}{2\delta x}\right)(u_{i-1} - u_i)$$

. Thus a Reynolds number based on the local mesh spacing, $Re_{local} = |a|\,\delta x/\mu$ can be defined. It can be easily proved if $Re_{local} \leqslant 2$ , then $f$ will be monotonically increasing or decreasing. In this case the viscosity is enough to dissipate the unphysical oscillations. Inspired by the analysis, the physical viscosity is introduced into the current implementation of WENO algorithm by the modification to $\epsilon$. First the Reynolds number based on the local mesh spacing is computed and if $Re_{local}$ is lower than a pre-defined threshold, the flow region near this part is denoted as diffusion-controlled and linear reconstruction instead of the WENO algorithm is used. In the current work the threshold Reynolds number is taken to be 5. Then for the rest of the domain, $\epsilon$ is re-defined as

$$\epsilon' = \epsilon + \frac{0.1}{Re_{local}}$$

. With the use of $Re_{local}$, in domains dominated by viscous effects, the admissible variations is enlarged and the WENO weights tend to the designed optimal value and higher accuracy can be achieved. For high Reynolds number flows, at least in the viscous sub-layer, no WENO reconstruction is used and reconstruction order is forced to be the designed value and this would yield better accuracy for the boundary layer and this also results in a bit cost saving by the way. In the off-body part of the flow, although the turbulent viscosity is much bigger than the molecular viscosity, the mesh spacing is much larger, thus in this part $Re_{local}$ is seldom a small value and the physical viscosity has limited ability to suppress the oscillations. While on the other hand with the development of computation resources, larger scale and denser mesh is used to resolve the flow problem, so the $Re_{local}$ is decreasing with denser mesh and physical viscosity has increasing capability of suppressing oscillations. It has to be noted there maybe a better formulation to bring in the viscous effect and the approach in this work is just heuristic.

With the calculated $W^L_{i+1/2}$ and $W^R_{i+1/2}$, throughout this paper the HLLC Riemann flux[10] is used to compute the inviscid flux across the cell interface. For viscous cases, second order scheme is used to discrete the viscous term. For turbulent cases, the two equation Menter-SST turbulence model[11] is used to calculate the turbulent viscosity. Unless otherwise stated, the computation throughout this paper is conducted with multiblock body-fitted structured mesh and Alternating Direction Implicit (ADI) method with three levels of multigrid are used for the time integration.

## 3. Numerical example: NACA 0012 airfoil

The NACA-0012 airfoil case is solved with the Building Cube Method[12,13]. In the Building Cube Method block structured Cartesian mesh is used to discretize the flow region and all the blocks have the same number of points. Ghost cells are used to exchange information between neighbor blocks. This test case is conducted in the two-dimensional inviscid mode and within the current Building Cube Method, ghost cell based Immersed Boundary method[14] is used to treat solid walls not aligned with the mesh lines. Fifth order WENO method is used for the inviscid fluxes. A five stages explicit Runge-Kutta time marching method and the Full Approximation Scheme (FAS) type multigrid method are used to integrate the governing equation towards convergence.

First the case with inflow Mach number $M_\infty = 0.8$ is tested. For this case the shock wave is approximately aligned with the mesh lines. Both the primitive variable based WENO and the characteristic variable based WENO are computed. Also in order to test the sensitivity of the convergence to the small number $\epsilon$,

both $\epsilon = 10^{-2}$ and $\epsilon = 10^{-6}$ are tested. The comparison of convergence histories are given in Fig. 4. Of all the four WENO reconstruction strategies, for both choices of the small value $\epsilon$, the characteristic variable based WENO method yields smooth convergence. For the primitive variable approach, with $\epsilon = 10^{-2}$ the convergence speed is similar as that for the characteristic based approach, while with $\epsilon = 10^{-6}$ the residual has been reduced about three orders of magnitude and then fails to converge any more.

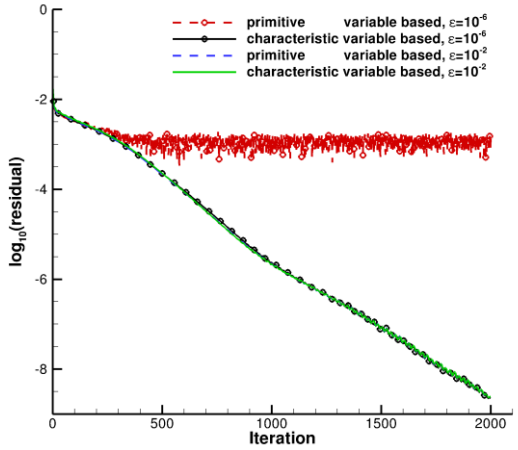


Fig. 4 Comparison of convergence histories for various WENO strategies for the NACA-0012 case, $M_\infty = 0.8$

In order to compare the characteristic and primitive strategies, the WENO weights used to calculate $u^L_{i+1/2}$ in the region contains the shock wave are compared. According to the comparison, in the characteristic variable based reconstruction, only the component corresponding to the downstream propagating pressure wave demonstrates large variations. The first and the third component yield moderate variations across the shock. In this case the shock wave is approximately aligned with the mesh lines, thus the component related to the transverse velocity has minor change across the shock and the WENO weights for the fourth component approach the designed value. The simplified version of characteristic variable based WENO is thus reasonable and the component representing the vortex wave can be linear interpolated without harming the shock capturing. In the primitive variable based reconstruction, the nonlinear process selecting the smoothest candidate stencils are activated at more grid points and also all weights demonstrate larger variations, in other words, the primitive variable approach tends to apply lower order reconstruction to more grid points. The entropy distributions are compared in Fig. 5 and Fig. 6.

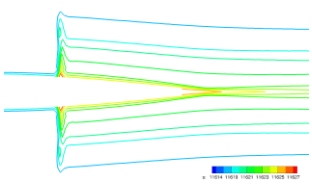

Fig. 5 Entropy distribution, the characteristic variable based reconstruction

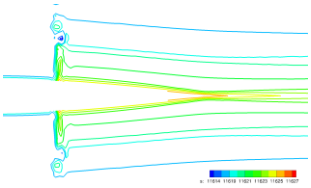

Fig. 6 Entropy distribution, the primitive variable based reconstruction

With the characteristic reconstruction the entropy rise across the shock wave is sharply and monotonically captured, while there are entropy oscillations with the primitive reconstruction.

Another case with the incoming Mach number $M_\infty = 0.99$ is simulated with both the characteristic and primitive variable based reconstruction. The small number $\epsilon$ has two choices, $10^{-2}$ and $10^{-6}$. Also the simplified WENO reconstruction with $\epsilon = 10^{-2}$ is tested. In this case the shock wave is not aligned with the mesh lines and the shock extends further into the ambient and a much larger computational domain is used. The comparison of convergence histories is given in Fig. 7. As shown in Fig. 7, only the two characteristic variable based reconstructions with $\epsilon = 10^{-2}$ reduce the residuals smoothly and the other three result in convergence stall. While even with $\epsilon = 10^{-6}$ the characteristic WENO has better convergence than the primitive counter part.

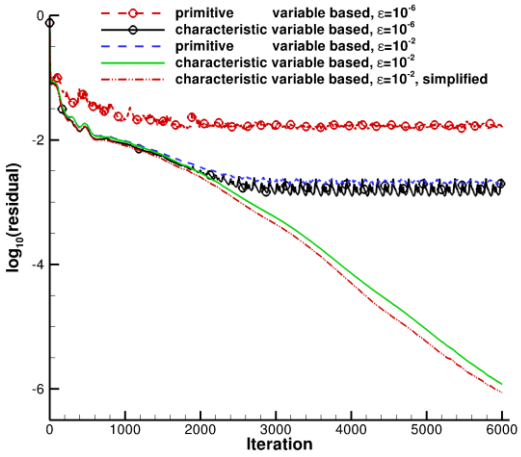


Fig. 7 Comparison of convergence histories for various WENO strategies for the NACA-0012 case, $M_\infty = 0.99$

The computational results are compared in Fig. 8 and Fig. 9. The simplified characteristic variable based WENO sharply captures the shock wave. In this case the angle between the shock front and the mesh line is about $40^o$, while from the convergence history and the density contour, the simplified version still works well and yields similar results as the original version. A significant difference can be observed that the numerical result obtained with primitive variable based WENO contains post-shock oscillations while the oscillations in the former two methods are much smaller. Based on the numerical results from the NACA-0012 case, the characteristic variable based WENO reconstruction has better convergence speed and accuracy, thus should be preferred.

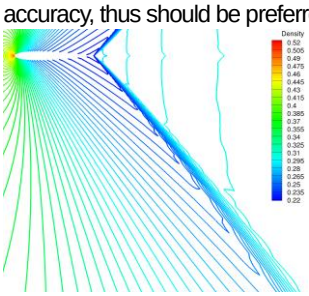

Fig. 8 Density distribution, the simplified characteristic variable based reconstruction

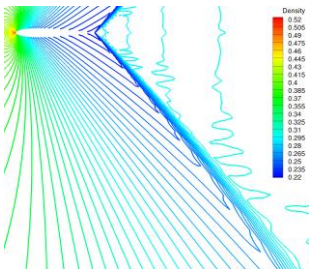

Fig. 9 Density distribution, the primitive variable based reconstruction

## 4. Numerical example: RAE 2822 airfoil

To examine the performance of the WENO reconstruction for transonic and turbulent flows, the RAE2822 airfoil is simulated with fifth order WENO reconstruction. In this case, the mesh consists of $369 \times 65$ grid points. The freestream condition considering wind tunnel correction is $\alpha = 2.54^{\circ}, M_{\infty} = 0.734$ and the Reynolds number is $Re = 6.5 \times 10^{6}$.

With $\epsilon = 10^{-2}$, three sets of numerical experiments have been conducted, including the characteristic variable based, the primitive variable based and the simplified characteristic variable based WENO reconstructions. Note that the $Re_{local}$ based correction is absent in these three computations. As shown in Fig. 10, similar as in the NACA-0012 case, for $\epsilon = 10^{-2}$ all the three WENO reconstructions demonstrate smooth convergence. To further examine the behavior of these reconstruction methods $\epsilon$ is set to a stringent value of $10^{-12}$ and the residuals are shown in Fig. 11. In this situation, both characteristic variable based WENO methods successfully converge with minor loss of speed. While the residual of primitive variable based WENO fluctuates at the level of about $10^{-5}$.

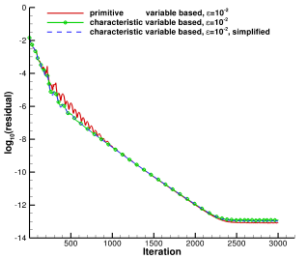


Fig. 10 Comparison of convergence histories of various WENO strategies, $\epsilon = 10^{-2}$

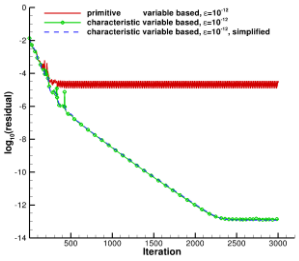


Fig. 11 Comparison of convergence histories of various WENO strategies, $\epsilon = 10^{-12}$

By carefully monitoring the residuals at all mesh points, it is found the convergence degradation takes place in the wake region. In this area the Mach number is about 0.5 and there are large variations of both primitive and characteristic variables and the mesh spacing is much larger than in the boundary layer. As analyzed in the above, in this case the physical viscosity is not enough to fully damp the variations. While in this case the characteristic variable based approach behaves better and still converges successfully. From the NACA-0012 case and the RAE2822 case the convergence speed of the characteristic based method is better and less sensitive to the small value $\epsilon$.

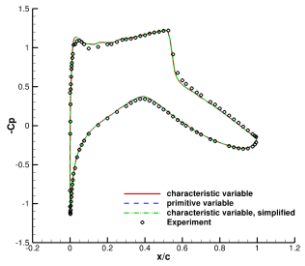


Fig. 12 Comparison of surface pressure coefficients, $\epsilon = 10^{-2}$

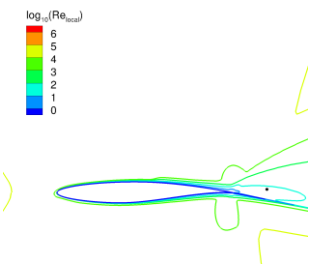


Fig. 13 Computed Reynolds number based on the local mesh spacing

The surface pressure coefficients are compared in Fig. 12. All the results are in good agreements with the experiment, though they have different convergence properties. The computation results with the primitive variables based WENO are shown in Fig. 13 and the black dot in every picture denotes the grid point with maximum residual. In two dimensions there are two values of $Re_{local}$ and the minimum of the two are shown in Fig. 13. The turbulent viscosity reaches its maximum near this point and thus $Re_{local}$ has a rather small value of 50. Another set of numerical experiments are conducted to examine the effect of bringing in viscous parameter into the WENO reconstruction. Both $\epsilon = 10^{-12}$ and $\epsilon = 10^{-2}$ are tested. Also the calculations with and without the viscous correction are conducted.

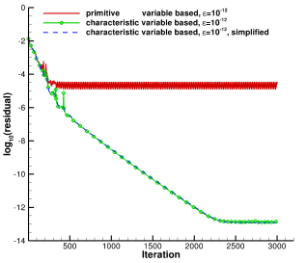


Fig. 14 Convergence histories with and without viscous effect in the primitive variable based WENO, $\epsilon = 10^{-12}$

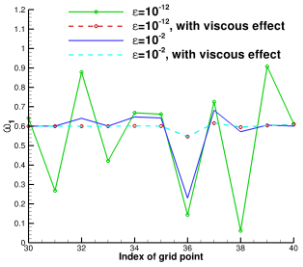


Fig. 15 WENO reconstruction weights along the I=const mesh lines in the wake region, $\omega_1$ for the velocity-Y component

According to the convergence histories in Fig. 14, with the effect of $Re_{local}$, the convergence behavior has been greatly improved as in this situation the effective value of $\epsilon$ is significantly magnified. For $\epsilon = 10^{-2}$, taking into account of $Re_{local}$ has little effect on the convergence, while the accuracy has been obviously improved. The WENO reconstruction weights of $\omega_1$ corresponding to the velocity-Y component are compared in Fig. 15. For both choices of $\epsilon$, the weights are tuned towards the designed value for optimal order of accuracy. Note that there are still some weights not equal to the designed value and the viscous effects can be further strengthened to deactivate the usage of the nonlinear interpolation for highest accuracy in this region, while at the risk of worse shock capturing and a better option is to increase the mesh resolution in the wake region.

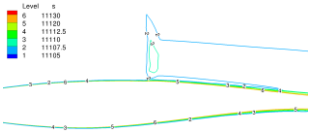

Fig. 16 Entropy distributions, simplified characteristic variable based WENO

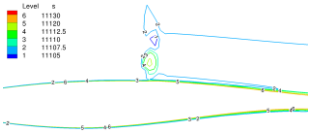

Fig. 17 Entropy distributions, primitive variable based WENO

For characteristic variable base WENO, the situation is similar as in the primitive variable based WENO with $\epsilon = 10^{-2}$. The convergence speed is less affected, while all the reconstruction weights are tuned towards the optimal value and thus the accuracy is improved in the wake region. With the viscous effect, the order of accuracy of WENO reconstruction in the boundary layer and the wake region is primarily determined by the viscous parameter $Re_{local}$. In the shock region, as the viscosity is in general much smaller, thus the WENO reconstruction weights still depend on the small value $\epsilon$. Similar as in the NACA-0012 case,

the characteristic variable based WENO has better accuracy and the primitive variable based WENO tends to activate the nonlinear interpolation at more grid points. The entropy distributions are compared in Fig. 16 and Fig. 17 and the characteristic variable approach has obviously better accuracy.

## 5. Numerical example: Rotor-37 compressor

The third test case is an example of the three dimensional flow through the transonic compressor NASA Rotor-37. This compressor rotor is widely used to test the numerical algorithms and to study the complex flow phenomena of compressor aerodynamics. Plentiful of flow features important to the engineering community co-exist in the Rotor-37 case, such as strong shock wave-boundary layer interaction induced flow separation, tip vortex and vortex-shock wave interactions. Thus the capturing of detailed flow features demands accurate algorithms. On the other hand because of the strong adverse pressure gradient and the complex flow structures in this case, it is hard to guarantee the convergence and stability of high order schemes. So in the literature central scheme with artificial dissipation, also third order MUSCL reconstruction are mostly used in this case and fifth order WENO type high order scheme is seldom tested.

In this work the fifth order WENO reconstruction is tested, both in the primitive based and the simplified characteristic based styles. The small number is set to $\epsilon = 10^{-2}$ and the viscous effect is included. The grid used in this case is a multiblock structured mesh and consists of approximately 1M points. The spacing between the solid and the first off-wall point is tuned to guarantee the $y^+$ is roughly 1. One-dimensional distribution of total temperature, total pressure and the flow angles at the inlet surface are treated with the use of 1D Riemann invariants. At the outlet surface, static pressure distribution based on the radial equilibrium equation is used.

| Order | Primitive variable | Characteristic variable | Characteristic variable, simplified |
|---|---|---|---|
| 3 | 1.00 | 1.78 | 1.37 |
| 5 | 1.62 | 3.28 | 2.06 |

Table. 1 CPU cost of various WENO strategies

For this three dimensional case, third order WENO and fifth order characteristic variable based WENO are also executed for several steps to assess the CPU cost of various WENO strategies, as shown in Table. 1. Note that the CPU time for third order primitive variable based WENO reconstruction is set to be the reference value and also this CPU time is not the total CPU time, but the one elapsed in the reconstruction step. From the comparison, the simplified version of characteristic based WENO developed in this work dramatically reduces the CPU cost. For a general purpose solver, there are moreover several CPU-extensive procedures, such as the time marching, Riemann flux and the solution of turbulence equation. Thus accompanied with the CPU time reduction comes from the simplified version, the total CPU cost overhead is about $5\%$ compared to the primitive variable based approach.

The convergence histories of both WENO strategies are compared in Fig. 18. For the primitive variable based approach, the residual is reduced from $10^{-3}$ to about $2 \times 10^{-6}$ and then stalls. With the simplified characteristic variable based reconstruction, the residual can be further reduced to about $6 \times 10^{-10}$.

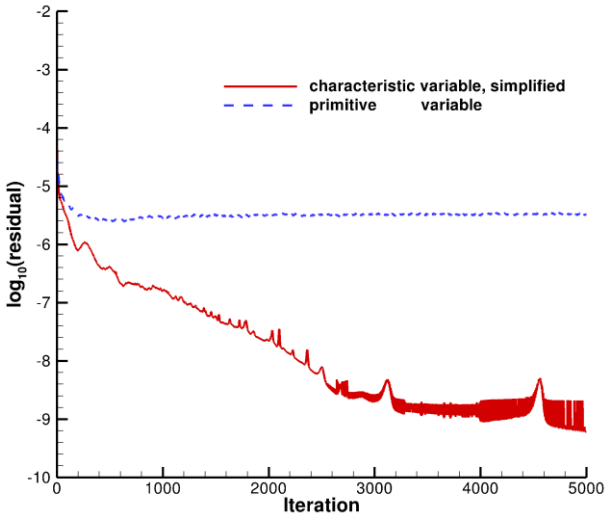


Fig. 18 Convergence histories of fifth order WENO reconstruction for the Rotor-37 test case

In order to assess the actual reconstruction order of the WENO algorithm in practical engineering problems, a parameter in the form of

$$\delta\omega = \max_k \frac{|\omega_k - \omega_{k,optimal}|}{\omega_{k,optimal}}$$

is used to reflect the deviation of the interpolation weight from its designed optimal value. The larger of this value, the lower reconstruction order of accuracy is used. The distributions of $\delta\omega$ at the radial position of $50\%$ blade height are given in Fig. 19 and Fig. 20.

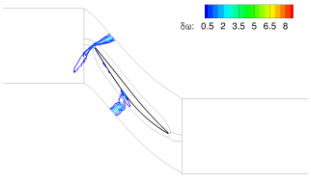

Fig. 19 Distribution of $\delta\omega$, simplified characteristic variable based WENO

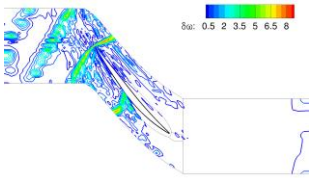

Fig. 20 Distribution of $\delta\omega$, primitive variable based WENO

From Fig. 19 the nonlinear interpolation process is activated only in the regions of leading edge shock and the passage shock in the simplified characteristic variable based WENO. While as shown in Fig. 20, besides the shock region, the nonlinear interpolation is used at more grid points in the primitive variable approach. An interesting phenomenon is in the region from trailing edge to the outlet in Fig. 20, the use of nonlinear interpolation is suppressed and it is attributed to the inclusion of viscous effect, as in this region the turbulent viscosity is much larger and $Re_{local}$ is between 10 and 100.

The vorticity magnitudes based on the relative velocity at the axial positions of $10\%$ chord and $50\%$ chord are compared in Fig. 21 and Fig. 22. At the $10\%$ chord, both methods yield approximately the same tip vorticity, while at downstream position, the vorticity is dissipated quicker in the primitive variable based

approach, especially the suction-side tip vortex.

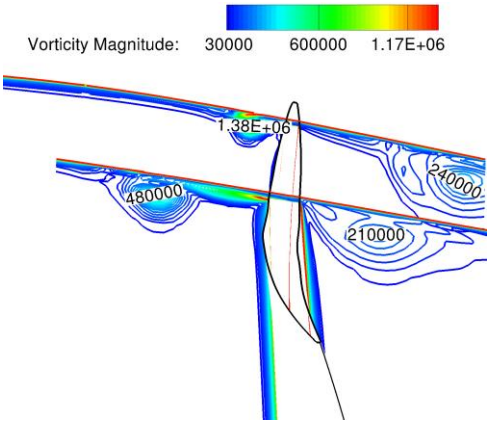


Fig. 21 Vorticity magnitude distributions at axial positions of $10\%$ chord and $50\%$ chord, simplified characteristic variable based WENO

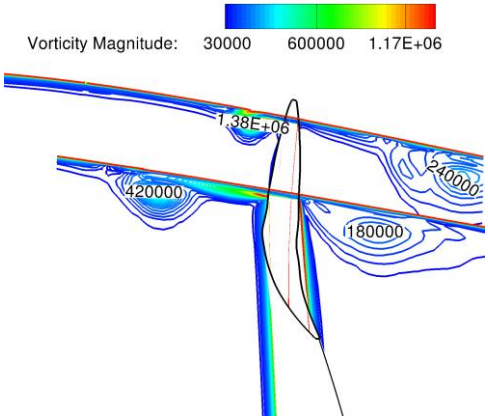


Fig. 22 Vorticity magnitude distributions at axial positions of $10\%$ chord and $50\%$ chord, primitive variable based WENO

The evolution and the breakdown of the tip vortex are important to the stability of the compressor and thus the accurate prediction is necessary. From the comparison the characteristic variable based WENO reconstruction gives better accuracy and efficiency and should be preferred.

6. Numerical example: DLR F4 wing-body

The following test case is the DLR F4 wing-body configuration. The flow conditions used is $M_\infty = 0.75, \alpha_\infty = -0.4^o$and the Reynolds number $Re = 3 \times 10^6$ based on the wing's mean aerodynamic chord length. The mesh consists of about 3.3M grid points and is provided by the workshop committee. Note that this standard mesh is of questionable quality with high skewness in the near-wall region.

Fifth order WENO reconstruction with both the simplified characteristic variable and primitive variable based reconstructions are used. Also the $Re_{local}$ based viscous correction is used to reflect the viscous effect in the reconstruction.

For this case, as given in Fig. 23, the WENO reconstruction gives reasonable convergence speed, though the grid has a low quality. The two reconstructions have similar convergence properties and give the same lift coefficients. While the drag coefficient using the primitive variable based approach is about 1.5 counts higher.

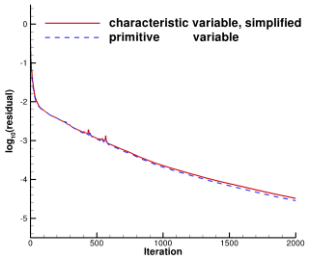


Fig. 23 Convergence histories of the DLR F4 wing-body case

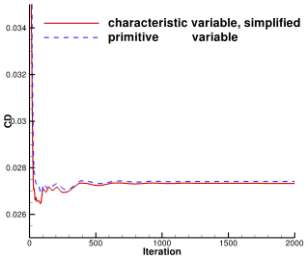


Fig. 24 CD convergence of the DLR F4 wing-body case

The comparison of the isosurface with $\delta\omega = 1$ is given in Fig. 25 and Fig. 26. From the isosurface in Fig. 25, in the simplified characteristic variable based reconstruction, the nonlinear interpolation is activated near the windshield, the leading edge of the wing and trailing edge and also in a small part of the tip vortex. While a significant difference can be observed in the far-field. In the primitive variable approach the nonlinear interpolation is extensively used in the tip vortex region and the wake region. Thus although both methods yield similar lift and drag coefficients, the simplified characteristic variable based reconstruction better preserve the tip vortex along long distance because in this region highest order linear interpolation is always used. Thus for cases the tip vortex is important, such as the helicopter flows[9], using characteristic variable would help to further improve the accuracy.

Fig. 25 $\delta\omega = 1$ isosurface, simplified characteristic variable based WENO

Fig. 26 $\delta\omega = 1$ isosurface, primitive variable based WENO

7. Conclusions

In this work the application of high order WENO scheme to engineering problems is studied. In the literature it is believed for engineering problems, the use of characteristic variable in the high order WENO reconstruction has little superiority, while at the gainless cost of CPU overhead. Thus for engineering problems the primitive variable or conservative variable is always used. In this paper, the choice of variable is found to do play a role in terms of accuracy and convergence. Also the CPU time overhead can be obviously reduced based on some reasonable simplifications. From the work in this paper the following conclusions can be made:

(1). For engineering problems, the characteristic variable based WENO has better accuracy and the nonlinear interpolation procedure is always sharply activated near the discontinuities. While in the primitive variable based approach it tends to activate the nonlinear interpolation at more grid points and thus the reconstruction accuracy is lower. As a result the characteristic

variable based WENO has better capability of monotone capture of shock wave and better preserves detailed flow features.
(2). For engineering problems in the subsonic and transonic regimes, the CPU overhead of the characteristic based WENO can be obviously reduced. Based on the Rankine-Hugoniot conditions, the components of characteristic variable corresponding to vortex wave can be linear interpolated without visible loss of shock capturing capability.
(3). The characteristic variable based WENO has better convergence issue and is less sensitive to the small number $\epsilon$. The improved convergence speed can somewhat counteract the CPU time overhead in the characteristic variable based WENO.
(4). For viscous case, it is preferred to take into account the viscous effect. With modification to the small number $\epsilon$, in the viscous dominated region, the reconstruction order is tuned towards the designed value. Also the convergence speed can be improved with the consideration of viscous effect.

## 8. Acknowledgement

This work was supported by JSPS KAKENHI(21226018).

## Bibliography

(1) Bram Van Leer, “Towards the ultimate conservative difference scheme III. upstream-centered finite-difference schemes for ideal compressible flow”, Journal of Computational Physics, 23 (1991), pp. 263-275.
(2) Xu-Dong Liu, Stanley Osher, and Tony Chan, “Weighted essentially non-oscillatory schemes”, Journal of Computational Physics, 115 (1994), pp. 200--212.
(3) Guang Shan Jiang and Chi Wang Shu, “Efficient implementation of weighted ENO schemes”, Journal of Computational Physics, 126 (1996), pp. 202-228.
(4) Sergio Pirozzoli, “Numerical methods for high-speed flows”, Annual Review of Fluid Mechanics, 43 (2011), pp. 163-194.
(5) Yu-Xin Ren, Miao er Liu, and Hanxin Zhang, “A characteristic-wise hybrid compact-WENO scheme for solving hyperbolic conservation laws”, Journal of Computational Physics, 192 (2003), pp. 365--386.
(6) Shuhai Zhang and Chi-Wang Shu, “A new smoothness indicator for the WENO schemes and its effect on the convergence to steady state solutions.”, Journal of Scientific Computing, 31 (2007) , pp. 273--305.
(7) Robert H. Nichols, Robert W. Tramel, and Pieter G. Buning, “Evaluation of two high-order weighted essentially nonoscillatory schemes”, AIAA Journal, 46 (2008), pp. 3090--3102.
(8) Yiqing Shen, Gecheng Zha, and Baoyuan Wang, “Improvement of stability and accuracy for weighted essentially nonoscillatory scheme”, AIAA Journal, 47 (2009), pp. 331--344.
(9) Thomas H. Pulliam, “High order accurate finite-difference methods: as seen in OVERFLOW”, AIAA-2011-3851, 2011.
(10) P. Batten, M. A. Leschziner, and U. C. Goldberg, “Average-state Jacobians and implicit methods for compressible viscous and turbulent flows”, Journal of Computational Physics, 137 (1997), pp. 38--78.
(11) F. R. Menter, “Two-equation eddy-viscosity turbulence models for engineering applications”, AIAA Journal, 32 (1994), pp. 598--1605.
(12) Kazuhiro Nakahashi, “High-density mesh flow computations with pre-/post-data compressions”, AIAA-2005-4876, 2005.
(13) Kazuhiro Nakahashi, Aya Kitoh, Yuta Sakurai, and Matthias Meinke, “Three-dimensional flow computations around an airfoil by building-cube method”, AIAA-2006-1104, 2006.
(14) Rajat Mittal and Gianluca Iaccarino, “Immersed boundary methods”, Annual Review of Fluid Mechanics, 37 (2005), pp. 239--261.